Available online at www.sciencedirect.com
ScienceDirect
Current Opinion in Structural Biology

Junction-forming aquaporins

Andreas Engel[1,5], Yoshinori Fujiyoshi[2,5], Tamir Gonen[3,5] and Thomas Walz[4,5]

Aquaporins (AQPs) are a family of ubiquitous membrane channels that conduct water and solutes across membranes. This review focuses on AQP0 and AQP4, which in addition to forming water channels also appear to play a role in cell adhesion. We discuss the recently determined structures of the membrane junctions mediated by these two AQPs, the mechanisms that regulate junction formation, and evidence that supports a role for AQP0 and AQP4 in cell adhesion.

Addresses
[1] Maurice E. Mueller Institute, University of Basel, Biozentrum, Klingelberstrasse 70, CH-4056 Basel, Switzerland
[2] Department of Biophysics, Faculty of Science, Kyoto University, Oiwake, Kitashirakawa, Sakyo-ku, Kyoto 606-8502, Japan
[3] Department of Biochemistry, University of Washington, 1705 NE Pacific Street, Seattle, WA 98195, USA
[4] Department of Cell Biology, Harvard Medical School, 240 Longwood Avenue, Boston, MA 02115, USA

Corresponding author: Walz, Thomas (twalz@hms.harvard.edu)
[5] All the authors contributed equally to this review.

Current Opinion in Structural Biology 2008, **18**:229–235

This review comes from a themed issue on
Macromolecular assemblages
Edited by Edward Egelman and Andrew Leslie

Available online 14th January 2008

0959-440X/$ – see front matter

DOI 10.1016/j.sbi.2007.11.003

Structure and function of aquaporins (AQPs)

Members of the aquaporin (AQP) family have traditionally been divided into two classes, the AQPs, pure water channels that only conduct water, and the aquaglyceroporins, channels that also conduct small, uncharged solutes, most notably glycerol. In addition, AQPs also conduct a variety of other molecules, including larger solutes (AQP9 [1]), anions (AQP6 [2]), arsenite (AQP7 and AQP9 [3]), and presumably gases such as ammonia and carbon dioxide (e.g. AQP1, reviewed in [4]). In plants, AQPs that conduct hydrogen peroxide, boron, and silicon have also been described (reviewed in [5]). Although differing greatly in their channel specificities, all AQPs are strictly impermeable to protons thus protecting the transmembrane proton gradient. The first AQP structures determined were those of human aquaporin AQP1 [6] and the *Escherichia coli* aquaglyceroporin GlpF [7]. These and subsequent structural studies (reviewed in [8]) together with molecular dynamic simulations (reviewed in [9]) provided much insight into the structural basis for channel specificity and the proton exclusion mechanism of AQPs. AQP0 and AQP4 are different from other AQPs in that they not only form water channels but also appear to have another, very different function, namely a role in cell adhesion.

Aquaporin-0

Originally named MIP for major intrinsic polypeptide, AQP0 is the most abundant membrane protein in lens fiber cells [10]. It is present in single membranes but is particularly enriched in the 11–13-nm thin junctions, which feature orthogonal arrays [11]. Initially, much interest was focused on the role of AQP0 in membrane junctions, and reconstitution of purified AQP0 into liposomes showed that it caused the vesicles to cluster [12]. Once AQP1 was shown to be a water channel [13], functional studies on AQP0 shifted toward its channel characteristics (e.g. [14,15]). Still, interest in the adhesive properties of AQP0 re-emerged when two-dimensional (2D) crystallization experiments resulted in single-layered as well as double-layered crystals, which were analyzed by electron crystallography and atomic force microscopy (AFM) [16,17].

Several lines of evidence suggest that it is proteolytic cleavage that induces AQP0 to form junctions. In young fiber cells of the lens cortex, AQP0 exists as a full-length protein of 26 kDa. As fiber cells grow older and become buried deeper in the lens core, some of the AQP0 is proteolytically cleaved in an age-dependent manner (e.g. [18]). Early experiments showed that mild trypsin digestion of isolated lens membranes increases the number of AQP0 arrays [19]. However, as thin junctions are more abundant in the lens core [11], where the proportion of cleaved AQP0 is higher, protein cleavage also appeared a likely cause for junction formation. This hypothesis was experimentally tested by *in vitro* proteolysis of purified protein as well as AQP0 2D arrays [20•]. When detergent-solubilized, full-length AQP0 (26 kDa) was treated with chymotrypsin, the resulting 22-kDa fragment eluted at a higher molecular weight from a sizing column than full-length AQP0, suggesting that cleaved AQP0 tetramers form pairs. Furthermore, while electron micrographs of proteoliposomes containing full-length AQP0 isolated from the lens cortex showed individual, evenly dispersed vesicles (Figure 1a), exposure of these vesicles to chymotrypsin resulted in substantial clustering of the vesicles (Figure 1b). Proteoliposomes containing a mixture of both full-length and truncated AQP0 isolated from the lens core also clustered (Figure 1c). Finally, 2D crystallization of full-length AQP0 isolated from the lens cortex yielded single-layered sheets (Figure 1d), whereas the mixture of full-length and truncated AQP0 isolated from

Figure 1

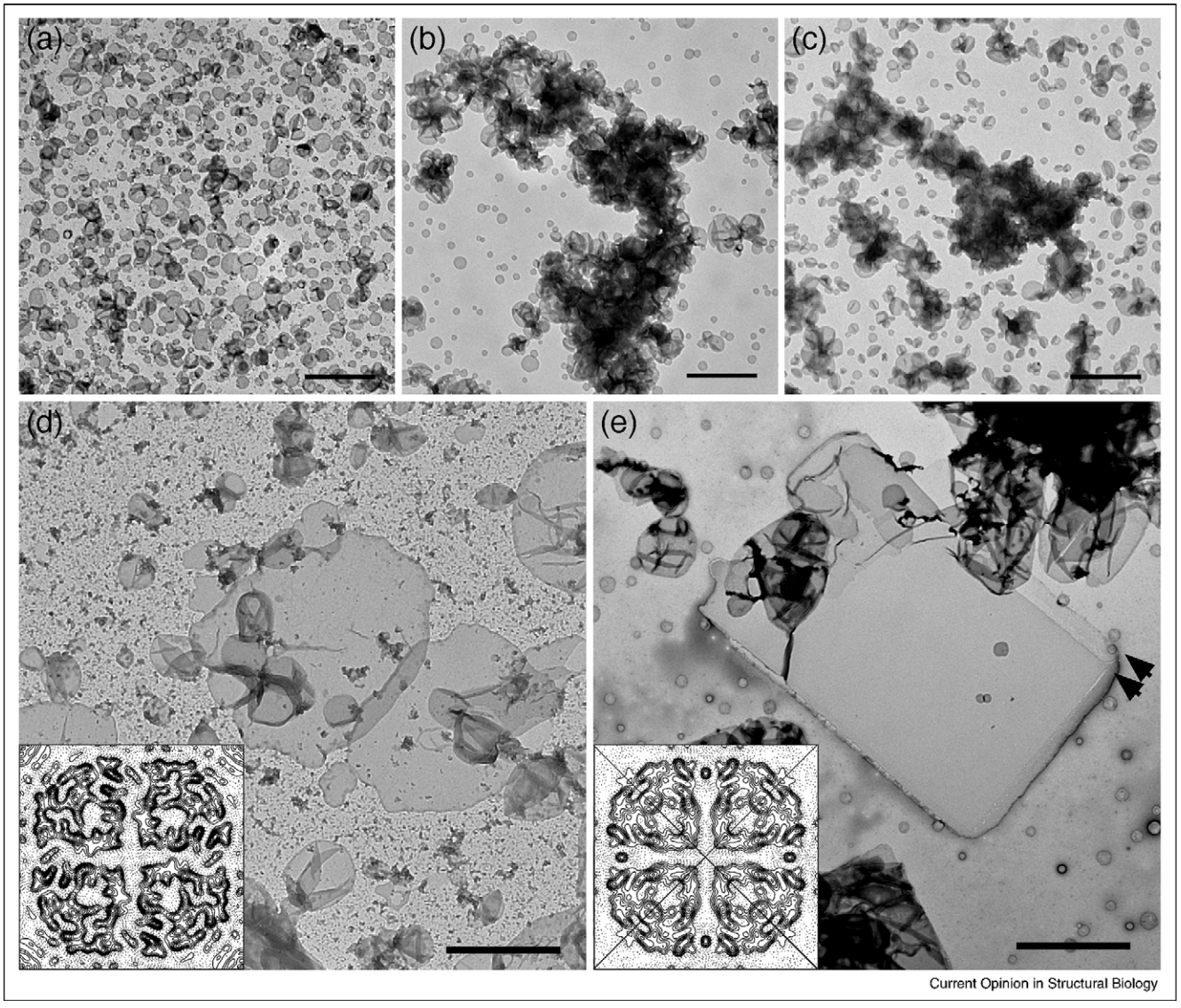

Cleavage of the cytoplasmic termini of AQP0 enhances the adhesive properties of its extracellular surface. **(a)** Proteoliposomes containing full-length AQP0 isolated from the lens cortex are uniformly distributed. **(b)** Treatment of the proteoliposomes shown in (a) with chymotrypsin causes the vesicles to cluster. **(c)** Proteoliposomes containing a mixture of full-length and truncated AQP0 isolated from the lens core cluster in a similar way as the proteoliposomes containing full-length AQP0 that were treated with chymotrypsin. **(d)** Reconstitution of full-length AQP0 isolated from the lens cortex produces single-layered 2D crystals. The inset shows a 4-Å projection map of an AQP0 tetramer in the single-layered crystals. **(e)** Reconstitution of a mixture of full-length and truncated AQP0 isolated from the lens core produces double-layered 2D crystals. The arrowheads indicate the edges of the two crystal layers. The inset shows a 4-Å projection map of two stacked AQP0 tetramers in the double-layered crystals. The diagonal black lines indicate the two mirror axes that result from the opposite orientations of the two interacting crystal layers. The scale bars in panels (a)–(e) correspond to 1 μm. The insets in (d) and (e) show complete unit cells with lattice constants of $a = b = 65.5$ Å. Adapted from [20•], with permission from Elsevier.

the lens core produced double-layered sheets (Figure 1e). All these results thus support the notion that proteolytic cleavage increases the propensity of AQP0 to form junctions.

The double-layered 2D crystals made it possible to determine the structure of junctional AQP0 by electron crystallography, first at 3-Å resolution [21] and then at 1.9-Å resolution [22••] (Figure 2). The lattice parameters of $a = b = 65.5$ Å and the thickness of about 11 nm of the double-layered AQP0 2D crystals are essentially the same as the dimensions of thin junctions between lens fiber cells [23], indicating that the crystals are a close representation of the *in vivo* junctions. The density map

Figure 2

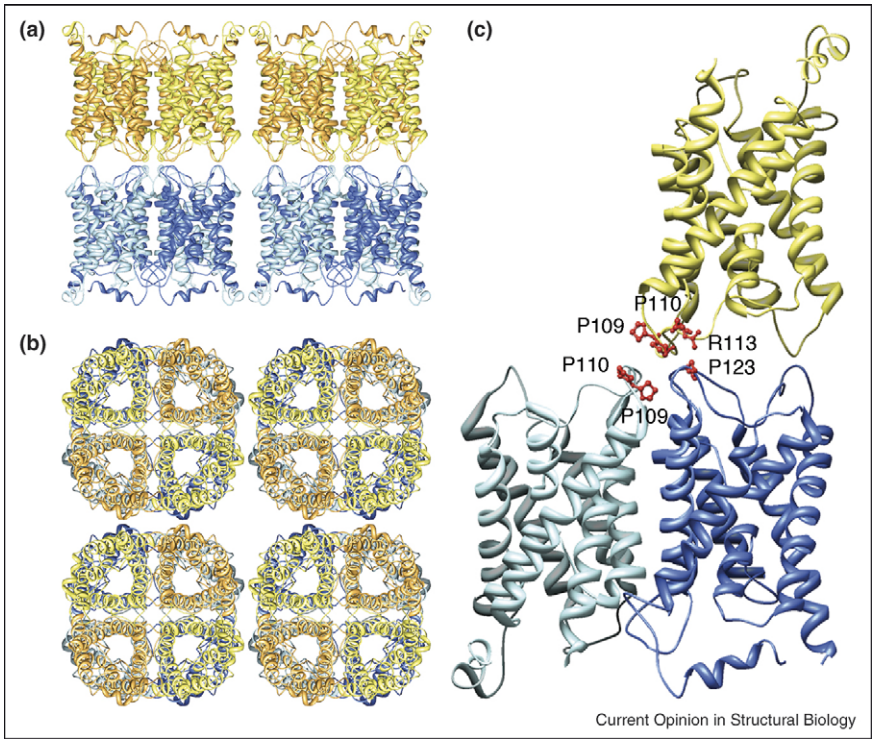

Double-layered 2D crystals formed by AQP0 (pdb accession code: 2B6O) [22••]. **(a)** View parallel and **(b)** view perpendicular to the membrane plane showing that the AQP0 tetramers in the two membrane layers are exactly in register. **(c)** Interactions between AQP0 tetramers formed by extracellular loop C. The proline–proline motif (Pro109 and Pro110) in loop C in the AQP0 monomer in the top layer (yellow) makes interaction with the proline–proline motif in an AQP0 monomer in the bottom layer (light blue). In addition, Arg113 in loop C in the AQP0 monomer in the top layer (yellow) makes interaction with Pro123 in loop C in another AQP0 monomer in the bottom layer (dark blue).

resolved only three water molecules in the water pathway that were also too far apart to form hydrogen bonds and thus suggested that the channel was in a closed conformation. Junction formation is the likely cause for channel closure because proteolytic cleavage does not affect the water permeability of AQP0 [24]. The formation of membrane junctions thus appears to convert AQP0 from a water pore to a pure adhesion molecule. The use of the same protein for different purposes is not uncommon in the lens and is known as gene sharing [25]. The density map also revealed nine lipid molecules per AQP0 monomer, illustrating one of the advantages of 2D crystals for structure determination of membrane proteins (reviewed in [26]). The structure of full-length AQP0 was independently determined to 2.2-Å resolution by X-ray crystallography, revealing the structure of nonjunctional AQP0 in the open conformation [27•]. The availability of atomic models for junctional, closed AQP0 in a lipid bilayer and nonjunctional, open AQP0 in a detergent micelle provided a wealth of information. For example, pore closure could be assigned mainly to a conformational change in the side chain of pore-lining residue Met176, which upon junction formation obstructs the water pore [22••]. The two structures also provided insight into the effects of lipids and detergents on the protein structure [28].

Unlike most other AQPs, AQP0 is not glycosylated and features a shortened extracellular loop A between the first two membrane-spanning α-helices [21,22••,27•]. These adaptations allow tetramers from adjoining membranes to make direct contacts through corresponding extracellular loops A and C. The contacts formed by residues in loop C, involve a Pro–Pro motif (Pro109 and Pro110), which is part of a one-turn helix (helix HC), and residues Arg113 and Pro123 (Figure 2c). Although loop C is in a virtually identical conformation in junctional and nonjunctional AQP0, cleavage of the cytoplasmic tails seems to correlate with a rearrangement in loop A [22••]. In the loop conformation of nonjunctional AQP0, Pro38 is at some distance from the center of the tetramer (Figure 3a). In addition, Trp34 lies above the pore and projects outward, blocking the approach of a second tetramer, and Arg33 is positioned in between two monomers. In the junctional AQP0 tetramer, loop A has reconfigured, positioning Pro38 so that it can form a rosette-like structure at the center of the tetramer (Figure 3c) and mediate a major

Figure 3

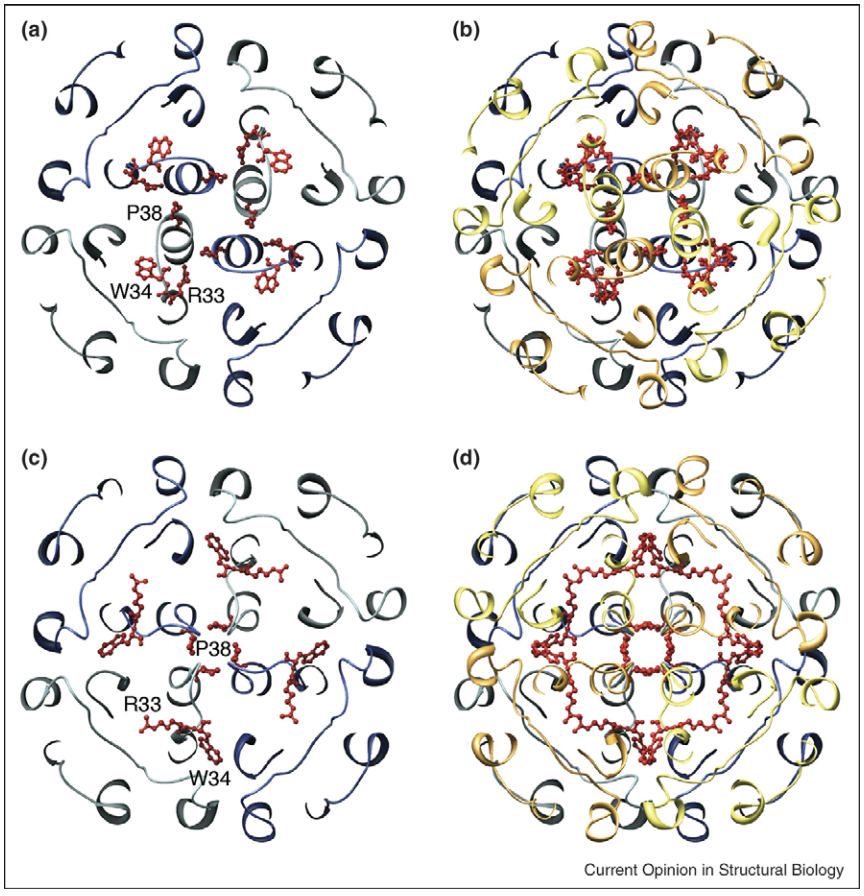

Two different conformations of AQP0's extracellular loop A and the resulting interactions in paired tetramers. **(a)** Conformation of loop A in the 2.2-Å X-ray structure of full-length AQP0 (pdb accession code: 1YMG) [27•]. Pro38 points away from the center of the tetramer, Trp34 lies above the pore and projects outward, blocking the approach of a second tetramer, and Arg33 is positioned in between two monomers. **(b)** The conformation of loop A in the paired tetramers seen in loosely packed 3D crystals of full-length AQP0 is the same as in (a), because the 2.2-Å X-ray structure of full-length AQP0 was used to obtain this low-resolution molecular replacement solution, but the two tetramers are rotated with respect to each other by 24° (pdb accession code: 2C32) [29•]. **(c)** Conformation of loop A in the double-layered 2D crystals (pdb accession code: 2B6O) [22••]. Pro38 forms a rosette-like structure at the center of the tetramer, and the side chains of Arg33 and Trp34 have swapped positions (compare with panel a). **(d)** In the completed junction, residues Pro38, Arg33, and Trp34 interact with the corresponding residues from the opposing tetramer.

junctional contact (Figure 3d). The side chains of Arg33 and Trp34 also swap positions, so that Trp34 no longer interferes with the close approach of another tetramer. In the completed junction, all three residues interact with the corresponding residues from the opposing tetramer (Figure 3d). AFM was used to image the extracellular surface of junctional AQP0 arrays [30•]. Membranes were isolated from the lens core and the AFM tip was used to remove the top layer from junctional membrane patches, which made it possible to image the extracellular surface of AQP0 arrays. The averaged surface topograph was more consistent with the conformation of loop A seen in the double-layered 2D crystals than in the 3D crystals, lending support to the notion that the conformation of loop A is the cause for junction formation rather than being induced by the interaction between tetramers in adjoining membranes, which were removed by the AFM tip before imaging. Loosely packed 3D crystals of full-length AQP0 also revealed paired tetramers [29•]. In these 3D crystals, the interacting tetramers were not exactly aligned as in the double-layered 2D crystals but rotated with respect to each other by 24°, resulting in different interactions between the tetramers (Figure 3b). These interactions can only form between isolated AQP0 tetramers but not between tetramers that are part of orthogonal arrays in adjoining membranes.

Aquaporin-4

AQP4, the predominant water pore in brain [31,32], is expressed in glial cells. It forms orthogonal arrays *in vivo*, which are particularly prominent in glial end feet surrounding vascular capillaries [33]. AQP4 is also expressed

in glial lamellae of the hypothalamus [34], where it may play a role in osmo-sensing, thermo-sensing, and glucose-sensing [32,35]. AQP4 exists in two splicing isoforms, one starting with Met1 (AQP4M1) and the other with Met23 (AQP4M23) [36,37]. It is predominantly, or possibly only, the shorter splicing variant AQP4M23 that assembles into orthogonal arrays, whereas the longer splicing variant AQP4M1 has little propensity to form arrays [38].

2D crystals obtained with recombinant AQP4M23 were double-layered but the distance and relative orientation of the two membranes in the double-layered 2D crystals varied slightly, complicating the electron crystallographic structure determination [39••]. The structure at 3.2-Å resolution revealed that AQP4 tetramers in the two membranes interact with each other through their extracellular surfaces (Figure 4a). Rather than being exactly stacked, as in the case of AQP0 (Figure 2a,b), the AQP4 tetramers are shifted so that a tetramer in one membrane is at the center of four tetramers in the adjoining membrane (Figure 4a,b). AQP4 features a short 3_{10} helix in extracellular loop C, helix HC, which contains the two residues, Pro139 and Val142, that mediate the interactions between opposing tetramers (Figure 4c). An isolated pair of interacting tetramers is unlikely to mediate significant adhesion because an AQP4 monomer in one membrane makes contact with only one subunit in a tetramer in the opposing membrane. In the 2D crystals each AQP4 tetramer interacts, however, with four tetramers in the adjoining membrane, so that an orthogonal array would significantly enhance AQP4-mediated adhesion. The variations in the relative positions of the two layers in the crystals suggest, however, that even crystalline AQP4 arrays promote only weak adhesion.

Unlike AQP0, AQP4 had not previously been implicated in cell adhesion, and the interactions between AQP4 tetramers in adjoining membranes are apparently weak. It was therefore of interest to understand whether the double-layered 2D crystals were just a result of the *in vitro* 2D crystallization of AQP4 or whether AQP4 could also form junctions *in vivo*, which would therefore be physiologically significant. When AQP4 was expressed in L-cells, a fibroblast cell line that does not express endogenous cell adhesion molecules, the cells showed some clustering, which was not observed when AQP1 was expressed [39••]. Second, thin sections through the hypothalamus revealed large membrane junctions between glial lamellae with short stretches of separated membranes. Although initial immunolabeling studies localized AQP4 to the separated membranes [34], subsequent studies also showed AQP4 in the junctional regions [39••]. These

Figure 4

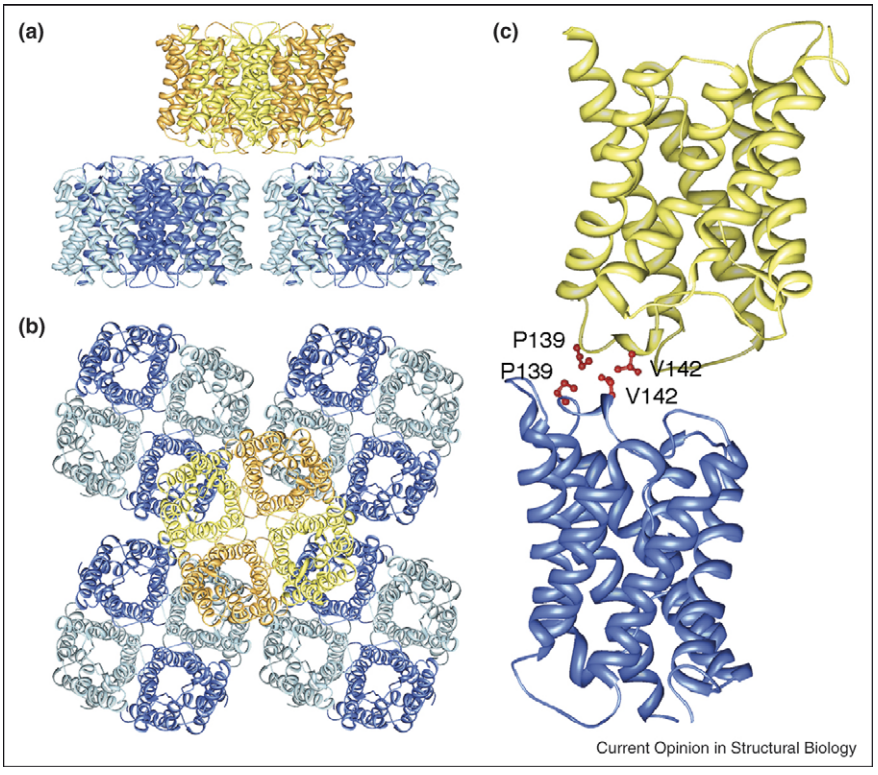

Double-layered 2D crystals formed by AQP4 (pdb accession code: 2D57) [39••]. **(a)** View parallel and **(b)** view perpendicular to the membrane plane showing that an AQP4 tetramer in one membrane layer makes interactions with four AQP4 tetramers in the other membrane layer. **(c)** Interactions between tetramers in the two layers are formed by residues Pro139 and Val142 in AQP4's extracellular loop C.

Table 1

Similarities between the junction-forming water channels AQP0 and AQP4

AQP0	AQP4
AQP0 is expressed as full-length protein, while shorter species are formed by age-dependent proteolysis (e.g. [18])	AQP4 is expressed as a long splicing variant, AQP4M1, and a short splicing variant, AQP4M23 [36]
Cleavage does not affect water permeability characteristics of AQP0 [24]	AQP4M1 and AQP4M23 have presumably the same water permeability characteristics (not yet experimentally determined)
AQP0 forms orthogonal arrays *in vivo* (e.g. [11])	AQP4 forms orthogonal arrays *in vivo* [33]
Proteolytic cleavage increases the propensity of AQP0 to form orthogonal arrays [19]	Mainly (or possibly only) the shorter splicing variant of AQP4 forms orthogonal arrays [38]
AQP0 has been localized to thin junctions between lens fiber cells (e.g. [23])	AQP4 has been localized to junctions between glial lamellae in the hypothalamus [39••]
Reconstitution of AQP0 isolated from the lens core produces double-layered 2D crystals	Reconstitution of recombinant AQP4M23 produces double-layered 2D crystals
Junction formation closes the water channel in AQP0 [20•,22••]	Junction formation obstructs the extracellular channel entrance in AQP4 [39••]

results thus supported a possible role of AQP4 in junction formation *in vivo*. The physiological role of AQP4 junctions is still speculative, but they may be involved in osmoregulation [39••]. In the double-layered 2D crystals, the AQP4 molecules show a tight tongue-into-groove packing, which results in a partial blockage of the extracellular pore entrances. Formation of AQP4 junctions *in vivo* would thus potentially lead to a reduced water permeability of glial cell plasma membranes. Conversely, rapid water flow through the channels could drive the interacting membranes apart and thus resolve the junctions. As a result of the characteristics of AQP4, glial cells expressing a high ratio of AQP4M1 would produce small AQP4 arrays providing weak adhesion between membranes, which would easily separate and be sensitive to small water flows resulting from small osmotic differences. *Vice versa*, glial cells expressing a high ratio of AQP4M23 would produce large AQP4 arrays providing stronger adhesion between membranes that would withstand larger water flows associated with larger osmotic differences.

Conclusions

Despite differences in the specifics, there are striking parallels between AQP0 and AQP4, which may be characteristic of junction-forming AQPs (Table 1). Both proteins exist in a long and a short form, which result from proteolytic cleavage in the case of AQP0 and expression of two splicing variants in the case of AQP4. Both AQPs assemble into orthogonal arrays in native membranes, whereby the shorter protein species, especially in the case of AQP4, have a higher propensity to assemble into square arrays. Both proteins have been localized to membrane junctions that are most probably formed by the interaction of orthogonal arrays in the adjoining membranes. In the case of AQP0, junction formation appears to close the water channel, while in the case of AQP4 the water flow may regulate the adhesion. The consolidation of water permeation and cell adhesion in single membrane proteins, such as in AQP0 and AQP4, is intriguing. Therefore, the term 'adhennel' has been coined for membrane proteins that function both as a cell adhesion molecule and a membrane channel [39••]. Future experiments may identify further AQPs as adhennels. One possibility would be SoPIP2;1, which also forms double-layered 2D crystals upon reconstitution [40].

Acknowledgements

We thank Richard Hite for help with preparing the figures. Work in the Engel laboratory is supported by the National Center of Competence in Research for Structural Biology, SNF grant 3100-059415 to AE, and the NoE 3D-EM, EU project (LSHG-CT-2004-502828). Work in the Fujiyoshi laboratory is supported by Grants-in Aid for Specially Promoted Research, JST and NEDO in Japan. Work in the Gonen laboratory is supported by NIH grant R01 GM079233. Work in the Walz laboratory is supported by NIH grants P01 GM062580 and R01 EY015107.

References and recommended reading

Papers of particular interest, published within the annual period of review, have been highlighted as:

- • of special interest
- •• of outstanding interest

1. Tsukaguchi H, Shayakul C, Berger UV, Mackenzie B, Devidas S, Guggino WB, van Hoek AN, Hediger MA: **Molecular characterization of a broad selectivity neutral solute channel**. *J Biol Chem* 1998, **273**:24737-24743.

2. Yasui M, Hazama A, Kwon TH, Nielsen S, Guggino WB, Agre P: **Rapid gating and anion permeability of an intracellular aquaporin**. *Nature* 1999, **402**:184-187.

3. Liu Z, Shen J, Carbrey JM, Mukhopadhyay R, Agre P, Rosen BP: **Arsenite transport by mammalian aquaglyceroporins AQP7 and AQP9**. *Proc Natl Acad Sci U S A* 2002, **99**:6053-6058.

4. Cooper GJ, Zhou Y, Bouyer P, Grichtchenko II, Boron WF: **Transport of volatile solutes through AQP1**. *J Physiol* 2002, **542**:17-29.

5. Maurel C: **Plant aquaporins: novel functions and regulation properties**. *FEBS Lett* 2007, **581**:2227-2236.

6. Murata K, Mitsuoka K, Hirai T, Walz T, Agre P, Heymann JB, Engel A, Fujiyoshi Y: **Structural determinants of water permeation through aquaporin-1**. *Nature* 2000, **407**:599-605.

7. Fu D, Libson A, Miercke LJ, Weitzman C, Nollert P, Krucinski J, Stroud RM: **Structure of a glycerol-conducting channel and the basis for its selectivity**. *Science* 2000, **290**:481-486.

8. Gonen T, Walz T: **The structure of aquaporins**. *Q Rev Biophys* 2006, **39**:361-396.

9. de Groot BL, Grubmuller H: **The dynamics and energetics of water permeation and proton exclusion in aquaporins**. *Curr Opin Struct Biol* 2005, **15**:176-183.

10. Bloemendal H, Zweers A, Vermorken F, Dunia I, Benedetti EL: **The plasma membranes of eye lens fibres. Biochemical and structural characterization**. *Cell Differ* 1972, **1**:91-106.

11. Costello MJ, McIntosh TJ, Robertson JD: **Distribution of gap junctions and square array junctions in the mammalian lens**. *Invest Ophthalmol Vis Sci* 1989, **30**:975-989.

12. Dunia I, Manenti S, Rousselet A, Benedetti EL: **Electron microscopic observations of reconstituted proteoliposomes with the purified major intrinsic membrane protein of eye lens fibers**. *J Cell Biol* 1987, **105**:1679-1689.

13. Preston GM, Carroll TP, Guggino WB, Agre P: **Appearance of water channels in *Xenopus* oocytes expressing red cell CHIP28 protein**. *Science* 1992, **256**:385-387.

14. Mulders SM, Preston GM, Deen PM, Guggino WB, van Os CH, Agre P: **Water channel properties of major intrinsic protein of lens**. *J Biol Chem* 1995, **270**:9010-9016.

15. Nemeth-Cahalan KL, Hall JE: **pH and calcium regulate the water permeability of aquaporin 0**. *J Biol Chem* 2000, **275**:6777-6782.

16. Fotiadis D, Hasler L, Muller DJ, Stahlberg H, Kistler J, Engel A: **Surface tongue-and-groove contours on lens MIP facilitate cell-to-cell adherence**. *J Mol Biol* 2000, **300**:779-789.

17. Hasler L, Walz T, Tittmann P, Gross H, Kistler J, Engel A: **Purified lens major intrinsic protein (MIP) forms highly ordered tetragonal two-dimensional arrays by reconstitution**. *J Mol Biol* 1998, **279**:855-864.

18. Takemoto L, Takehana M, Horwitz J: **Covalent changes in MIP26K during aging of the human lens membrane**. *Invest Ophthalmol Vis Sci* 1986, **27**:443-446.

19. Kistler J, Bullivant S: **Lens gap junctions and orthogonal arrays are unrelated**. *FEBS Lett* 1980, **111**:73-78.

20. • Gonen T, Cheng Y, Kistler J, Walz T: **Aquaporin-0 membrane junctions form upon proteolytic cleavage**. *J Mol Biol* 2004, **342**:1337-1345.
This paper demonstrates that cleavage of the cytoplasmic termini of AQP0 enhances the adhesive properties of the extracellular side of AQP0, inducing the formation of membrane junctions.

21. Gonen T, Sliz P, Kistler J, Cheng Y, Walz T: **Aquaporin-0 membrane junctions reveal the structure of a closed water pore**. *Nature* 2004, **429**:193-197.

22. •• Gonen T, Cheng Y, Sliz P, Hiroaki Y, Fujiyoshi Y, Harrison SC, Walz T: **Lipid–protein interactions in double-layered two-dimensional AQP0 crystals**. *Nature* 2005, **438**:633-638.
This paper reports that the 1.9-Å structure of AQP0 obtained by electron crystallography of double-layered 2D crystals showed the conformational change in extracellular loop A and identified the junction-forming interactions between tetramers in adjoining membranes. The density map also revealed water molecules in the closed water channel and nine lipid molecules surrounding the AQP0 subunits.

23. Zampighi G, Simon SA, Robertson JD, McIntosh TJ, Costello MJ: **On the structural organization of isolated bovine lens fiber junctions**. *J Cell Biol* 1982, **93**:175-189.

24. Ball LE, Little M, Nowak MW, Garland DL, Crouch RK, Schey KL: **Water permeability of C-terminally truncated aquaporin 0 (AQP0 1-243) observed in the aging human lens**. *Invest Ophthalmol Vis Sci* 2003, **44**:4820-4828.

25. Piatigorsky J, Wistow GJ: **Enzyme/crystallins: gene sharing as an evolutionary strategy**. *Cell* 1989, **57**:197-199.

26. Hite RK, Raunser S, Walz T: **Revival of electron crystallography**. *Curr Opin Struct Biol* 2007, **17**:389-395.

27. • Harries WE, Akhavan D, Miercke LJ, Khademi S, Stroud RM: **The channel architecture of aquaporin 0 at a 2.2-Å resolution**. *Proc Natl Acad Sci U S A* 2004, **101**:14045-14050.
This paper reports that the structure of full-length AQP0 was determined by X-ray crystallography of 3D crystals and showed the conformation of extracellular loop A in nonjunctional AQP0, in which the water pore is in the open conformation.

28. Hite RK, Gonen T, Harrison SC, Walz T: **Interactions of lipids with aquaporin-0 and other membrane proteins**. *Pflugers Arch* 2007, in press. Q1

29. • Palanivelu DV, Kozono DE, Engel A, Suda K, Lustig A, Agre P, Schirmer T: **Co-axial association of recombinant eye lens aquaporin-0 observed in loosely packed 3D crystals**. *J Mol Biol* 2006, **355**:605-611.
This paper reports that loosely packed 3D crystals show that full-length AQP0 can also form pairs but the interactions between the tetramers are different from those seen in the double-layered 2D crystals.

30. • Buzhynskyy N, Hite RK, Walz T, Scheuring S: **The supramolecular architecture of junctional microdomains in native lens membranes**. *EMBO Rep* 2007, **8**:51-55.
This paper reports that AFM images of AQP0 junctions in isolated lens membranes support the notion that the conformational change in extracellular loop A is a prerequisite for junction formation and not the result of junction formation.

31. Hasegawa H, Ma T, Skach W, Matthay MA, Verkman AS: **Molecular cloning of a mercurial-insensitive water channel expressed in selected water-transporting tissues**. *J Biol Chem* 1994, **269**:5497-5500.

32. Jung JS, Bhat RV, Preston GM, Guggino WB, Baraban JM, Agre P: **Molecular characterization of an aquaporin cDNA from brain: candidate osmoreceptor and regulator of water balance**. *Proc Natl Acad Sci U S A* 1994, **91**:13052-13056.

33. Rash JE, Yasumura T, Hudson CS, Agre P, Nielsen S: **Direct immunogold labeling of aquaporin-4 in square arrays of astrocyte and ependymocyte plasma membranes in rat brain and spinal cord**. *Proc Natl Acad Sci U S A* 1998, **95**:11981-11986.

34. Nielsen S, Nagelhus EA, Amiry-Moghaddam M, Bourque C, Agre P, Ottersen OP: **Specialized membrane domains for water transport in glial cells: high-resolution immunogold cytochemistry of aquaporin-4 in rat brain**. *J Neurosci* 1997, **17**:171-180.

35. Amiry-Moghaddam M, Ottersen OP: **The molecular basis of water transport in the brain**. *Nat Rev Neurosci* 2003, **4**:991-1001.

36. Lu M, Lee MD, Smith BL, Jung JS, Agre P, Verdijk MA, Merkx G, Rijss JP, Deen PM: **The human AQP4 gene: definition of the locus encoding two water channel polypeptides in brain**. *Proc Natl Acad Sci U S A* 1996, **93**:10908-10912.

37. Neely JD, Christensen BM, Nielsen S, Agre P: **Heterotetrameric composition of aquaporin-4 water channels**. *Biochemistry* 1999, **38**:11156-11163.

38. Furman CS, Gorelick-Feldman DA, Davidson KG, Yasumura T, Neely JD, Agre P, Rash JE: **Aquaporin-4 square array assembly: opposing actions of M1 and M23 isoforms**. *Proc Natl Acad Sci U S A* 2003, **100**:13609-13614.

39. •• Hiroaki Y, Tani K, Kamegawa A, Gyobu N, Nishikawa K, Suzuki H, Walz T, Sasaki S, Mitsuoka K, Kimura K *et al.*: **Implications of the aquaporin-4 structure on array formation and cell adhesion**. *J Mol Biol* 2006, **355**:628-639.
This paper reports that reconstitution of recombinant AQP4 resulted in double-layered 2D crystals. The atomic model of AQP4 obtained by electron crystallography showed the junction-forming interactions. The paper also provides evidence that junction formation is a physiological role of AQP4.

40. Kukulski W, Schenk AD, Johanson U, Braun T, de Groot BL, Fotiadis D, Kjellbom P, Engel A: **The 5 Å structure of heterologously expressed plant aquaporin SoPIP2;1**. *J Mol Biol* 2005, **350**:611-616.